Unsteady Separation over Maneuvering Bodies

S. F. Shen* and Tzuyin Wu†
Cornell University, Ithaca, New York 14853

To understand unsteady separated flows over a maneuvering body requires an analysis of the Navier-Stokes equations in a set of body-fixed coordinates. Effects of the extra apparent body forces in various combinations are yet to be systematically explored. The boundary-layer equations in body-fixed coordinates, however, retain the usual form except for the Coriolis term which appears as the Rossby number in dynamic meteorology. In the two-dimensional case, the Coriolis term is absent. Computed results of the initiation of unsteady separation, according to the Lagrangian criterion, over a circular cylinder impulsively started into several variable motions, including acceleration, decleration, and rotation, are presented and discussed.

Nomenclature

A = fixed leading edge
e = eccentricity of rotation axis
$\boldsymbol{F}$ = apparent body-force vector, per unit mass
F = magnitude of vector $\boldsymbol{F}$
$\boldsymbol{F}'$ = resultant body-force vector defined in Eq. (6)
F' = magitude of vector $\boldsymbol{F}'$
$f(t)$ = time history of speed change in forward motion of a circular cylinder
$\boldsymbol{g}$ = gravitational acceleration vector
h_1, h_2, h_3 = stretch factors in mapping function, Eq. (11)
O = origin of body-fixed moving axes, usually at c.g. of aircraft
O' = origin of a set of inertial frame
p = pressure
$\boldsymbol{r}$ = position vector measured from O
$\boldsymbol{r}'$ = position vector measured from O'
t = time
t_1 = trigger time of speed change
$\boldsymbol{u}$ = velocity vector
u = velocity component in x direction
U = velocity component at edge of boundary layer, in x direction
U_0 = forward speed of cylinder in impulsive start case
v = velocity component in y direction
V = velocity component at edge of boundary layer, in y direction
x = body-fixed longitudinal coordinate; also, streamwise-coordinate for two-dimensional boundary layer
y = body-fixed lateral coordinate; also, normal coordinate for two-dimensional boundary layer
z = body-fixed coordinate normal to x and y directions
x', y', z' = a set of Cartesian coordinates for inertial frame
α, β = computational coordinates
δ = edge of boundary layer
Δ = time interval of speed change
θ = angular displacement due to rotation
ν = viscosity
ξ, η = Lagrangian coordinates for two-dimensional boundary layer
ρ = density
σ = arc length along the line of constant x
Ψ = azimuthal angle measured from fixed leading edge
$\boldsymbol{\Omega}$ = angular velocity vector of body motion
Ω = magnitude of vector $\boldsymbol{\Omega}$

Subscripts

A = aircraft
s = separation
t = time derivative
ξ, η = ξ, η derivatives

I. Introduction

WHEN vehicle behavior or its design is of interest, the forces and moments on an arbitrarily moving body are the needed inputs to the equations that govern the vehicle motion. In a flying aircraft, the aerodynamics as observed and experienced is most naturally expressed in terms of a set of body-fixed coordinates of the airplane. Any geometry change, due to control or structural deformation, as well as the rigid-body motion of the entire vehicle, can be specified conveniently by referring to these axes. Indeed, good dynamic characteristics of the airplane under its intended operational conditions are indispensable to successful design. "Dynamic stability," for instance, typically considers the small perturbations of an equilibrium configuration in level flight. The usual "stability derivatives" are based on assuming the perturbed aerodynamics as quasisteady, because of the relatively slow reaction time of conventional aircraft. For "flutter" analysis, on the other hand, larger "reduced frequencies" may be involved. In most treatments, a tacit assumption is that there is no significant separation of the boundary layer.

Experimental verifications of flows over moving bodies are fraught with difficulties. Ideally one should duplicate all the free-flight conditions. More commonly, however, the wind tunnel is used. As a persistent observer of unsteady aerodynamics for many years, Ericsson has repeatedly cataloged and discussed various anomalies of flows over moving bodies.[1,2] One of his main contributions is the emphatic dismissal of what he called the "free flight/wind tunnel equivalence" for any aerodynamic phenomenon where unsteady viscous effects, such as separation and reattachment of the boundary layer, play an essential role. Like Sears and Telionis[3,4] in proposing the M.R.S. (Moore-Rott-Sears) criterion for unsteady separation, Ericsson also brings attention to the "moving wall effect" on the asymmetric steady separation over a rotating cylinder in a uniform stream. In a different and intuitive

Received Aug. 22, 1988; revision received Nov. 9, 1989.

*John Edson Sweet Professor of Engineering.
†Graduate Research Assistant, Department of Mechanical Engineering.

manner, however, the moving wall effect has been used by Ericsson to explain qualitatively several perplexing observations. A clean example is the difference of two flows generated by an airfoil in a uniform stream, one from its oscillations in the plunging mode and the other from its oscillations in the pitching mode. Linearized inviscid theory predicts no difference, whereas experiment shows otherwise—because the boundary layer separates differently.

Ericsson's explanation was that the moving wall would promote or delay separation through adding or depleting the kinetic energy of the fluid particles adjacent to the wall. There is much truth in this mechanism. Attempts to account for nonstationary effects, e.g., by incorporating a time lag, are discussed in the most recent papers of Ericsson and Reding[5] and Ericsson.[6] Curiously and conspicuously missing, however, is any acknowledgment of the progress regarding the criterion for unsteady separation (such as the M.R.S.-criterion) in the last two decades. Without such a criterion, as far as detailed information from the analysis or simulation of boundary-layer flow with unsteady separation is concerned, Ericsson's moving wall effect is severely handicapped for quantitative predictions. In a semiempirical way, other ad hoc computations of unsteady separated boundary layers, including interaction with the inviscid flow, have been made, which despite simplifications, can be adjusted to show good correlation in specific cases. For the dynamic stall problem, see for example Jumper et al.[7,8]

However, if the body motion is arbitrary, it seems more appealing in the long run to follow a rational systematic treatment of the fluid dynamics with proper reference to the moving noninertial coordinates. In a straightforward manner, the Navier-Stokes equations can be written in the body-fixed coordinates of an arbitrarily moving aircraft, which contain inertial body-force terms representing linear and angular accelerations of the aircraft as well as the Coriolis and centripetal effects of its angular motion; see, e.g., Shen.[9] In principle, given a specific problem, the computation requires essentially the same code as the usual one without the body-force terms. More importantly, systematic analysis of these equations offers the possibility of gaining real insight into the highly complex phenomena, which can arise from the multitude of interactions of the various body-force terms. The Rossby number in dynamic meteorology, for example, has led to many consequences unfamiliar to aerodynamicists. It was also shown in Shen[9] that fortunately, the boundary-layer approximation in the moving coordinates turns out to be mathematically very much the same as in the usual case, provided the forcing terms are first evaluated at the edge of the boundary layer in terms of the (relative) velocity. The (relative) velocity must be brought to nil at the body surface with the help of the boundary layer. Thus, concepts and previous studies of the unsteady separation over a fixed wall can be directly extended to moving bodies, at least from the viewpoint of the boundary-layer approximation.

The boundary-layer approximation, in the limit of very large Reynolds number, is a valid simplification of the Navier-Stokes equations until separation intervenes. It meanwhile serves well as a diagnostic tool for separation, which identifies separation as a singularity not only in the well-known steady case but also in the unsteady case, according to the Lagrangian analysis of van Dommelen and Shen.[10,11] (In contrast with the Navier-Stokes solution at a finite Reynolds number, the sudden rapid thickening of the boundary layer associated with separation is exaggerated into a "virtual barrier" at the singularity.) Especially for motions which begin with a fully attached boundary layer, the time instant and the spatial location of the first appearance of separation can be unambiguously determined by computing the unsteady boundary layer in moving coordinates and using the Lagrangian criterion of singularity. The calculations in Shen[9] showed quantitatively the different separation behaviors over an airfoil oscillating in a freestream in the plunging mode and the pitching mode, influenced by additional parameters such as the pivot location, mean angle of attack, and the amplitude. The aerodynamic model was unrealistically crude, and mainly served to illustrate the methodology.

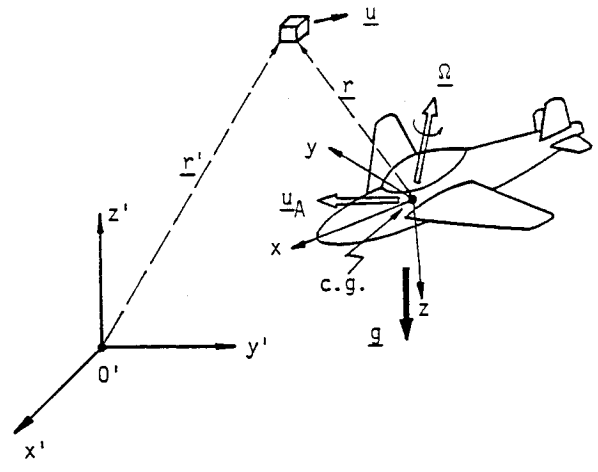

Fig. 1 General features of a body-fixed coordinates system.

In this paper, we present some more definitive results, obtained from accurate calculations of unsteady boundary-layer separation under the influence of body acceleration. To simplify the inviscid freestream, the study is focused on a circular cylinder impulsively started into different types of variable motion. The computation scheme is basically the two-dimensional Lagrangian code developed in van Dommelen and Shen[9,10] for a circular cylinder impulsively started to a constant velocity, now adapted for arbitrary history of translational and rotational plane motion. In the first problem, the translational motion includes rapid changes of the forward velocity to 50% larger and smaller values at different moments prior to the onset of separation. We next treat the motion involving both forward translation and rotation about different pivot points. (A short summary of the second case has been listed in Shen,[9] but without discussion.) These studies reveal important insights on the mechanism of unsteady separation, which conventional reasoning, largely based on experiences with steady separation in Eulerian description, do not seem to provide.

At this time, we can find no other computation or theoretical results to compare with our findings on the time and location of the first appearance of separation in the various cases. Also, we cannot identify experimental observations that have information on the initiation of separation at high Reynolds numbers. Of practical interest is the development of separation after its initiation. Our work so far is but the first stage needed for further explorations.

II. Statement of Problem and Governing Equations

We are interested in the fluid flow surrounding an aircraft, say, which may be rapidly maneuvering in an arbitrary manner. Conventional studies of fluid dynamics presuppose an inertial frame, but it is straightforward to recast the Navier-Stokes equations in a set of arbitrarily moving coordinates. Already given in Shen[9] and also available in other sources, for completeness and easy reference, they are listed once more as follows:

$$\frac{\partial \boldsymbol{u}}{\partial t} + \boldsymbol{u} \cdot \nabla \boldsymbol{u} = -\frac{1}{\rho} \nabla p + \nu \nabla^2 \boldsymbol{u} + \boldsymbol{F} + \boldsymbol{g} \tag{1}$$

$$\nabla \cdot \boldsymbol{u} = 0 \tag{2}$$

$$\boldsymbol{F} = -\left[\frac{\mathrm{d}\boldsymbol{u}_A}{\mathrm{d}t} + 2\boldsymbol{\Omega} \times \boldsymbol{u} + \boldsymbol{\Omega} \times (\boldsymbol{\Omega} \times \boldsymbol{r}) + \dot{\boldsymbol{\Omega}} \times \boldsymbol{r} \right] \tag{3}$$

where, as sketched in Fig. 1,

$\boldsymbol{u}_A$ = translational velocity of the aircraft
$\boldsymbol{\Omega}$ = angular velocity of the aircraft
$\boldsymbol{r}$ = position of vector of the fluid element measured from the origin, usually fixed at c.g. of aircraft
$\boldsymbol{F}$ = apparent body force per unit mass, as a result of body motion

We shall not go into general discussion of the various dimensionless parameters which may be formed to represent the preceding body-force terms. Suffice it to note that the linear acceleration/deceleration of the body appears as a favorable/unfavorable pressure gradient in the momentum equation. For this term alone, it should not be unreasonable to expect certain consequences by analogy. As a matter of fact, in an early paper on defining and formulating the question of laminar stability in time-dependent boundary layers,[12] the stabilizing/destabilizing effects of acceleration/deceleration have been explicitly demonstrated in a model problem. The work was motivated by the visualization experiment of the boundary layer over a flat plate moving forward under rapid deceleration.[13] There was, however, no follow-up definitive research.

For viscous flow with separation, the boundary-layer plays a central role, and analysis of the boundary layer equations is greatly simpler than that of the full Navier-Stokes equations. So long as the approximation is valid, the momentum equations are, in usual notation for boundary layers,

$$\frac{Du}{Dt} = \frac{\partial U}{\partial t} + U\frac{\partial U}{\partial x} + V\frac{\partial U}{\partial y} + F'_x + \nu\frac{\partial^2 u}{\partial z^2} \tag{4}$$

$$\frac{Dv}{Dt} = \frac{\partial V}{\partial t} + U\frac{\partial V}{\partial x} + V\frac{\partial V}{\partial y} + F'_y + \nu\frac{\partial^2 v}{\partial z^2} \tag{5}$$

where U and V are components of the local freestream velocity $\boldsymbol{U}$ tangent to the surface, and F'_x and F'_y are components of the body-force resultant

$$\boldsymbol{F}' = \int_\delta^z \frac{\partial}{\partial z}(\boldsymbol{F}+\boldsymbol{g})\,dz$$

By Eq. (3), it follows that

$$\boldsymbol{F}' = 2\boldsymbol{\Omega}\times(\boldsymbol{U}-\boldsymbol{u}) \tag{6}$$

As in the conventional case, the body-fixed boundary layer serves similarly to allow a smooth transition between the inviscid velocity at the edge of the boundary layer and that prevailing at the wall, say, according to the no-slip condition. The only extra term in the tangential momentum equation represents the Coriolis effect, arising from the component of the rigid-body rotation normal to the local wall. We note that for boundary layers over a rotating body, the rotating coordinates have been a common choice to simplify the statement of the boundary conditions. The problem defined by Eqs. (4–6) is but a more general version of the atmospheric boundary layer of meteorology subjected to the Coriolis effect due to Earth rotation. The very same Coriolis term appears also in the formulations of other familiar problems, such as the one due to von Kármán on the viscous flow over a rotating plate, as well as the boundary layers over a slender rotating blade studied by Fogarty,[14] Tan,[15] and others. Surely for three-dimensional boundary layers over arbitrarily moving bodies, the additional mechanism must be expected to generate a multitude of interesting novel aspects awaiting further investigation.

For two-dimensional plane flows, e.g., around an airfoil in arbitrary plane motion, the only body rotation comes from pitching, and there is no Coriolis effect on the boundary layer. In essence, the unsteady boundary layer can be solved as if in an inertial frame, provided an "effective pressure gradient" is used, which amounts to prescribing the relative velocity at the edge of the boundary layer. Such in fact has been common practice in dealing with this class of problems. It then follows that so long as the inviscid flow outside of the boundary layer is given or can be calculated, the unsteady boundary layer over moving bodies can be attacked by available methods developed for an inertial frame with a specified time-dependent velocity along the outer edge.

Consequently, we proceed to exploit the Lagrangian code developed originally for a two-dimensional body impulsively set into a constant forward motion by van Dommelen in his thesis.[11] The accuracy of the Lagrangian code to pinpoint incipient unsteady separation seems to be now beyond dispute. The excellent approximate integral method formulated by Matsushita et al.,[16] for example, established its validity by comparing results for an impulsively started circular cylinder against those in Ref. 10. So long as the potential flow can be prescribed, the Lagrangian code enables us to compute cases involving arbitrary cylinder motion, at least until the first appearance of unsteady separation. In the following, we present a few results which exhibit the influence of body motion on the naissance of separation occurring in the laminar boundary layer over a circular cylinder. These could also serve as benchmark cases for verifying simpler approximations.

III. Unsteady Separation Calculations of a Circular Cylinder Suddenly Started into Variable Motion

As a pilot study of the effects of body motion, we consider the simple geometry of a circular cylinder impulsively started into arbitrary plane motion. To compare against the results originally calculated by van Dommelen and Shen[10,11] the same length and time units are retained, so that the cylinder is of radius 1, impulsively started to a forward velocity U_0, at which speed the cylinder moves forward 1/2 radius after unit time. In the absence of other motion, unsteady separation was found to initiate at $t = 3.01$ and the location $x = 1.937$ from the leading edge along the circumference. To add now other motions, the same boundary-layer equations may be used except that the freestream should be the relative velocity.

In Lagrangian calculation of two-dimensional boundary layers, the unknowns are the displacement $x(\xi,\eta,t)$ along the surface and the streamwise velocity $u(\xi,\eta,t)$. In the (ξ,η) plane, the governing equations are

$$u_t = \left(\frac{\partial U}{\partial t} + U\frac{\partial U}{\partial x}\right) + x_\xi^2 u_{\eta\eta} - 2x_\xi x_\eta u_{\xi\eta} + x_\eta^2 u_{\xi\xi} - x_\xi u_\xi x_{\eta\eta} + (x_\xi u_\eta + x_\eta u_\xi)x_{\xi\eta} - x_\eta u_\eta x_{\xi\xi} \tag{7}$$

$$x_t = u \tag{8}$$

plus the continuity equation

$$x_\xi y_\eta - x_\eta y_\xi = 1 \tag{9}$$

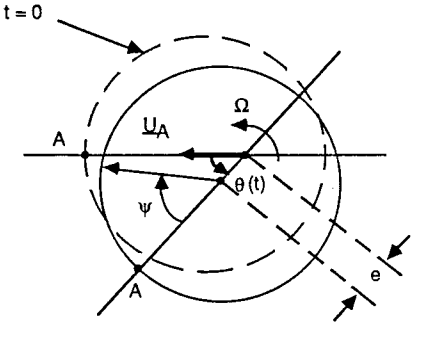

Fig. 2 Notations for a simultaneously translating and rotating cylinder.

to be integrated for y once x is determined at given t. The initial conditions are

$$t=0, \quad x=\xi, \quad y=\eta, \quad u=u_0(\xi,\eta)$$

and the no-slip condition may be cast as

$$t>0, \qquad x(\xi,0,t)-\xi=y(\xi,0,t)=0$$

Furthermore, there is the freestream condition:

$$y\to\infty,\ u\to U(x,t) \text{ given}$$

The computation domain is, for the cylinder in question, $0\le\xi\le 2\pi$, $0\le\eta$.

It may be useful to recall that the solution of Eq. (9) with $x(\xi,\eta,t)$ given is[10,11]

$$y=\int_0^{\sigma}\frac{d\sigma}{\sqrt{x_\xi^2+x_\eta^2}} \tag{10}$$

where σ is measured along the characteristic $x=$ const. The singularity occurring at $x_\xi=x_\eta=0$ pinpoints separation. Thus, from the Lagrangian analysis of unsteady boundary layer, separation occurs as the creation of a virtual barrier. A small fluid packet, centered at ξ_s, η_s, and of size $d\xi$, $d\eta$ initially, becomes deformed into a slice of no thickness upon reaching the location x_s at time t_s. Such an event is not possible with the full Navier-Stokes equation, but has been found to arise in the boundary-layer approximation with specified freestream. Basically, in contrast with conventional Eulerian separation criteria, which generally relate to certain features *at a point*, the Lagrangian criterion has to do with the behavior of a *packet* of fluid particles. It describes the ejection of boundary-layer fluid into the main stream by a straightforward mechanism. That the Lagrangian criterion needs only to find that zero of the gradient of the displacement $x(\xi,\eta,t)$, without having to cope with an emerging infinity, is an additional advantage in practical computation.

Now in body-fixed coordinates, it is convenient to refer the arbitrary cylinder motion to a translation of the pivot point about which the cylinder rotates (see Fig. 2). Let the translational velocity be U_A and angular velocity Ω, positive for counterclockwise rotation. The instantaneous potential flow outside the cylinder is determined by the component of the surface velocity normal to the surface. The boundary-layer coordinate along the surface, measured from the leading edge "A" which is fixed on the cylinder of radius 1, equals the azimuthal angle Ψ. If the cylinder already has an angular displacement $\theta(t)$ due to rotation, positive counterclockwise, we obviously should place the cylinder at an angle of attack $-\theta(t)$. The direction of the translation, in terminology of flight dynamics, is the "wind axis" pointing forward.

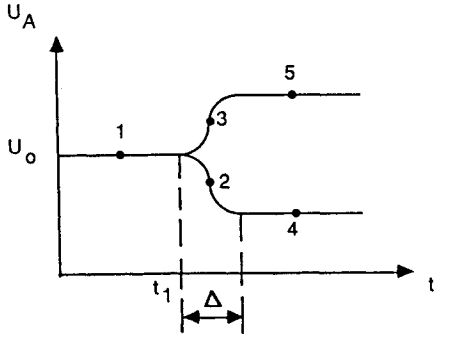

Fig. 3 Prescribed motion of a suddenly started cylinder with subsequent speed change.

It has proved to be helpful to map the computational domain into a unit square $0\le\alpha\le 1$, $0\le\beta\le 1$ by the following transformation:

$$\xi=\Psi=h_1\tan^{-1}\left(h_2\tan\frac{\pi\alpha}{2}\right)-h_3\alpha$$

$$\eta=1.5(4t/1+4t)^{1/2}\tan\frac{\pi\beta}{2} \tag{11}$$

Proper values of h_1, h_2, and h_3 are stretch factors chosen to improve local accuracy, e.g., near the front stagnation point. The time-dependent factor of β is to remove the singular behavior of the initial Rayleigh layer. The final basic equations, omitted here for brevity, are rewritten with α and β as the independent variables. The actual numerical solution has been carried out by approximating the terms with a Crank-Nicolson scheme, and the solver makes use of Gauss-Seidel iteration plus multigridding. Two specific types of variable motion have been studied, and the results are presented below.

A. Suddenly Started Cylinder with Subsequent Speed Change

Since linear acceleration acts like a constant pressure gradient in a body-fixed boundary layer, we examine first the effects of speed change after a cylinder has been started into forward motion. To avoid unnecessary and irrelevant singular behavior, the speed change is made in a fixed time interval and follows a smooth time history. Specifically, the body speed is prescribed to be

$$U_A=U_0, \qquad 0<t<t_1$$

$$U_A=U_0\left[1+\frac{1}{4}f(t)\right], \qquad t_1<t \tag{12}$$

As sketched in Fig. 3, we choose $f(t)$ to be

$$t_1<t<t_1+\Delta, \qquad f(t)=\pm\{1-\cos[\pi(t-t_1)/\Delta]\}$$

$$t_1+\Delta<t, \qquad f(t)=f(t_1+\Delta) \tag{13}$$

Thus, we have the freestream velocity for the boundary layer

$$U=2U_0\sin x, \qquad 0<t<t_1$$

$$=2U_0\left[1+\frac{1}{4}f(t)\right]\sin x, \qquad t_1<t \tag{14}$$

Table 1 Calculated results for a suddenly started circular cylinder with subsequent acceleration/deceleration in speed (mesh size 129 × 65 × 0.025)

	Deceleration				Acceleration			
	t_s	x_s	ξ_s	η_s	t_s	x_s	ξ_s	η_s
$t_1=1.5$ $\Delta=0.2$	3.41	1.74(99.7 deg)	1.29	0.68	2.75	1.99(114.0 deg)	1.65	0.43
$t_1=1.5$ $\Delta=1.0$	3.07	1.73(99.1 deg)	1.31	0.66	2.93	2.02(115.7 deg)	1.72	0.43
$t_1=2.5$ $\Delta=0.2$	3.01	1.78(102.0 deg)	1.52	0.54	3.05	2.06(118.0 deg)	1.68	0.58

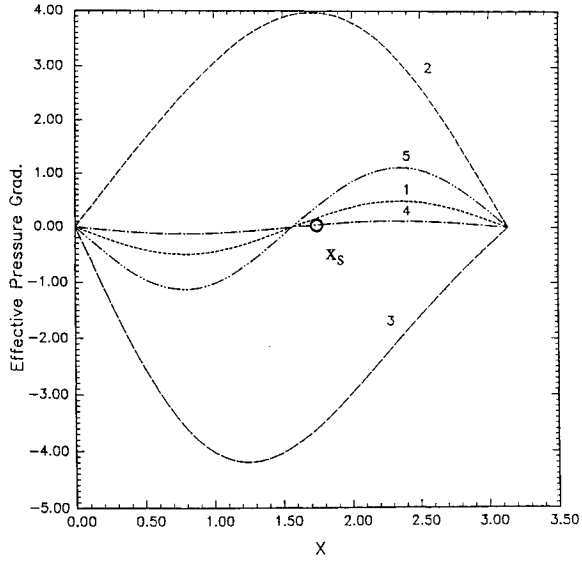

Fig. 4 Effective pressure gradient distribution at corresponding time designated as 1, 2, 3, 4, 5 in Fig. 3; $t_1 = 1.5$, $\Delta = 0.2$.

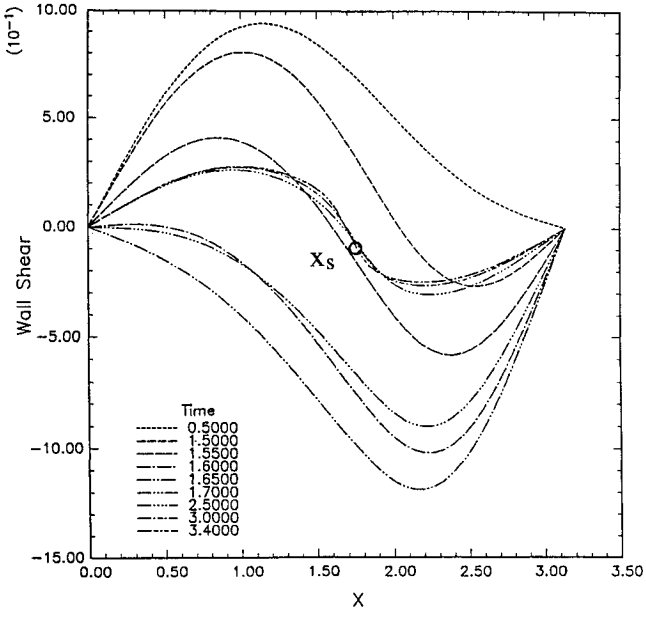

Fig. 5 Wall shear distribution ($t_1 = 1.5$, $\Delta = 0.2$, deceleration).

With the $\pm$ sign in the specified $f(t)$, both an acceleration and a deceleration case are covered. The standard case of van Dommelen and Shen corresponds to $f(t) = 0$.

Computations have been carried out for parameter values: $t_1 = 1.5$, $\Delta = 0.2$, and 1; $t_1 = 2.5$, $\Delta = 0.2$. In Table 1 are summarized the important results: the separation time t_s, the separation location (measured from the leading edge A) x_s, and the identity of the "separation center" (ξ_s, η_s). We note that without $f(t)$, separation occurs at $t_s = 3.01$, $x_s = 1.94$ (or 111 deg from the leading edge), with $\xi_s = 1.57$ and $\eta_s = 0.52$.

It is seen that regardless of the sign of speed change, in the case $t_1 = 2.5$ and $\Delta = 0.2$, the separation time t_s as well as the particle (ξ_s, η_s) remain close to the respective values for the case when no speed change is imposed. By advancing the trigger time t_1 to 1.5 and keeping $\Delta = 0.2$, the differences become larger. Interestingly, the separation time appears to be systematically delayed by deceleration and advanced by acceleration—seemingly contradictory to expectation. The location of separation, on the other hand, does tend to move toward the rear with acceleration and conversely with deceleration. These would become more mystifying if one tries to somehow relate separation with the instantaneous "effective pressure gradient"

$$\left.\frac{\partial p}{\partial x}\right|_{\text{eff}} = -(U_t + UU_x)$$

which for the case $t_1 = 1.5$ and $\Delta = 0.2$ is shown as Fig. 4. At $t = 1.6$ the effective pressure gradient distribution over a decelerated cylinder is given by curve 2 and seen to be much larger than the others. Yet separation is not initiated until $t = 3.41$. The corresponding effective pressure gradient distribution, at that time, is a considerably milder one, curve 4.

The notion of relating separation to flow reversal or instantaneous wall shear is equally untenable. The wall shear for all six cases have been computed, but only the deceleration case $t_1 = 1.5$, $\Delta = 0.2$ is shown in Fig. 5 as a representative. Separation starts at $t = 3.41$ and $x = 1.74$, Table 1, and is marked by O in both Figs. 4 and 5. (In Fig. 4, the curve 4 prevails for $1.7 < t < t_s$, while curve 1 corresponds to $t < 1.5$, and curve 2

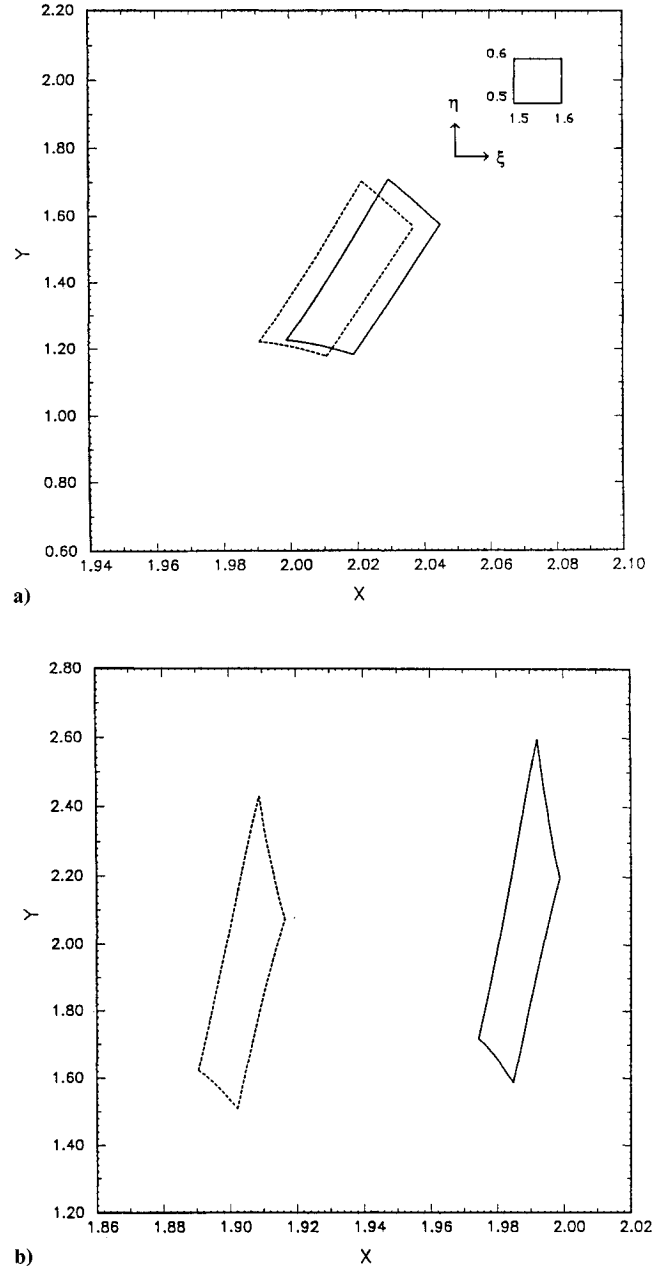

Fig. 6 Temporal evolution of a fluid packet under two different prescribed motions; —— constant speed motion, – – – with subsequent deceleration of $\Delta = 0.2$ triggered at $t_1 = 2.5$: a) $t = 2.6$; b) $t = 2.8$.

corresponds to $t = 1.6$; curves 3 and 5 are irrelevant for the case under consideration.) Note in Fig. 5 that the sign and magnitude of wall shear clearly are of no significance and, as shown in the figure, a reversed flow region is found to extend over the entire body for certain periods of time without provoking separation. A noticeable tendency in wall shear vs x to develop a front at separation is observed, however, consistent with the wave-steepening analogy suggested by Shen.[17] Of more interest is the bunching of the wall-shear curves as t_s is approached. Physically, the boundary layer is now splitting into two, sandwiched over a rapidly thickening middle layer of nearly constant velocity (or zero vorticity). The wall shear apparently changes little over a sizeable stretch bracketing the location $x = x_s$ for a significant amount of time (from $t = 2.5$ to $t = 3.41$) before separation erupts. The reversed flow and the negative wall shear are much stronger at $t = 1.7$, whereas the effective pressure gradient at $t = 1.7$ is already the same as the later ones (see Fig. 4). The dynamic process of separation is indeed difficult to explain in terms of these parameters.

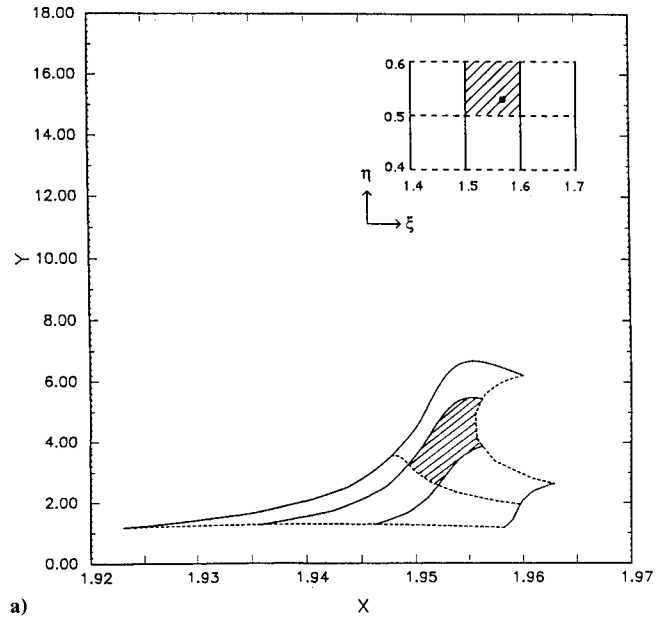

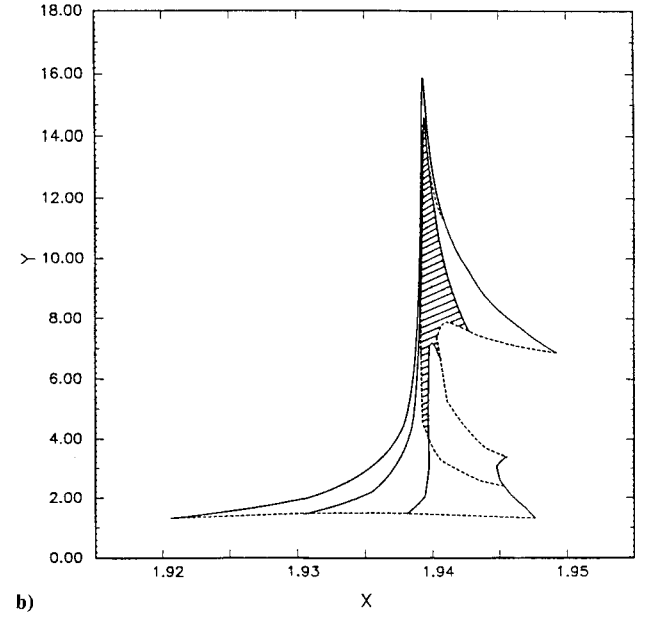

Fig. 7 Deformation of fluid packet close to separation; constant speed motion: a) $t = 2.95$, b) $t = 3$.

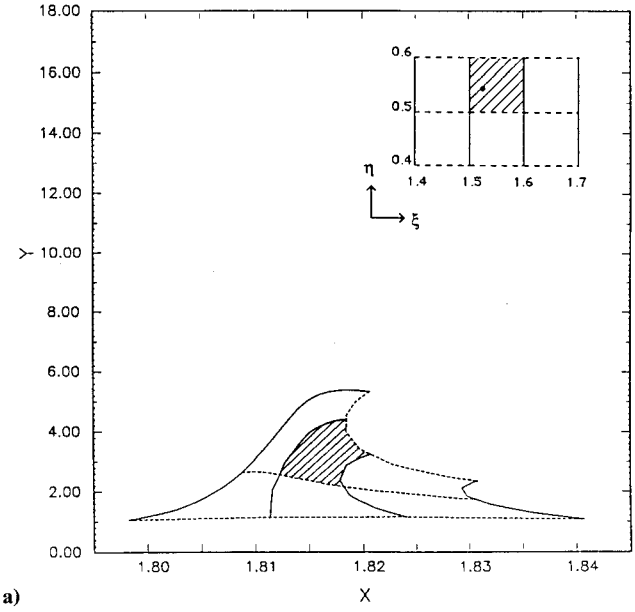

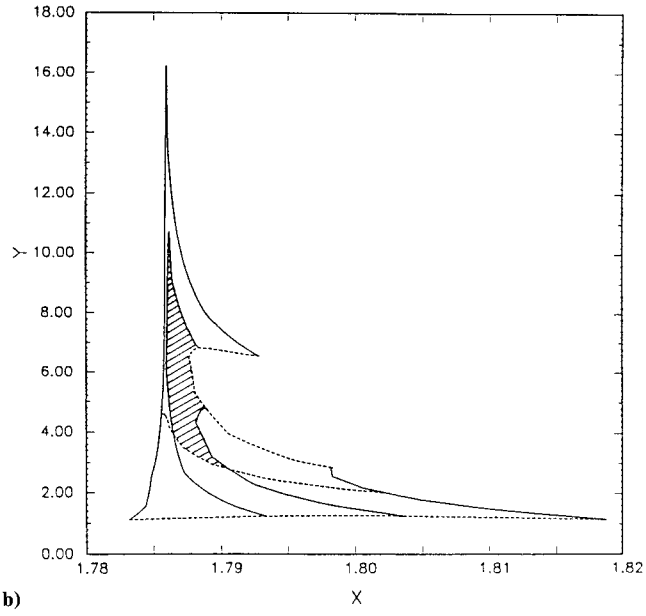

Fig. 8 Deformation of fluid packet close to separation; with deceleration of $\Delta = 0.2$ triggerted at $t_1 = 2.5$: a) $t = 2.95$; b) $t = 3$.

When we visualize a fluid packet away from the wall that evolves toward a singular behavior and initiates separation, the effects of sudden change of the body motion becomes more understandable. The pathology of separation may be revealed by examining the distortions of fluid packets in the (x,y) plane as influenced by various body motions. A comparison of the evolution of the same fluid packet (originally of square shape) under two different histories of motion, one with the standard impulsive start, the other with a subsequent deceleration triggered at $t_1 = 2.5$, is plotted in Fig. 6. As separation time is approached, both fluid packets become "steeper" and stretched in the y direction, but the shapes of the two elements remain quite similar at least until $t = 2.8$. (The position of the fluid packet relative to the body, at the same instant, is of course different.) This fact is interpreted as indicating that the fluid packet under consideration is essentially unaffected by the viscous effect emanating from the wall immediately after a rapid change in the motion of the entire fluid body. In other words, in the *inertial* frame, the sudden change in cylinder movement produces viscous action, which has to diffuse into the fluid through a Rayleigh layer mecha-

Table 2 Calculated results for a simultaneously translating and rotating circular cylinder (mesh size 65 × 65 × 0.025)

Ω:	−0.1			−0.5			0.0
e:	0.0	−0.4	−0.8	0.0	−0.4	−0.8	0.0
t_s	3.05	3.02	2.96	3.21	2.50	1.98	3.09
x_s	1.74	1.66	1.60	0.88	3.31	3.26	1.92
Ψ_s	99.7 deg	95.1 deg	91.7 deg	50.4 deg	189.6 deg	186.8 deg	110.1 deg
u_s	−0.35	−0.35	−0.36	−0.63	0.12	0.31	−0.27
ξ_s	1.39	1.31	1.25	0.91	3.73	3.69	1.53
η_s	0.60	0.59	0.59	1.07	0.39	0.38	0.55

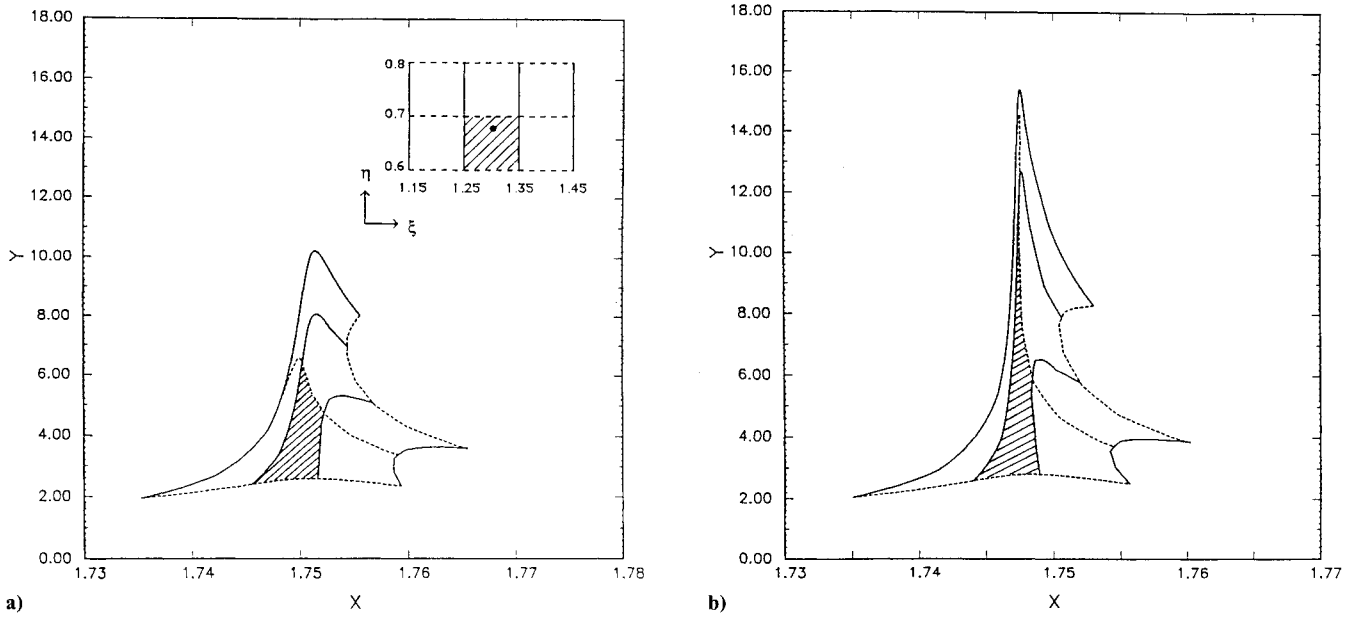

Fig. 9 Deformation of fluid packet close to separation; with deceleration of Δ = 0.2 triggered at $t_1 = 1.5$: a) $t = 3.35$; b) $t = 3.38$.

nism. Figures 7 and 8 exhibit the sudden "explosion," as the separation time draws near, of the shaded packet, which is initially a square mesh containing the separation center $(\xi_s \eta_s)$. A closer look shows that the upper halves of Figs. 7b and 8b are quite similar, but the bottom halves of the two structures bend in opposite directions. This illustrates that the viscous action resulting from changing the body motion is unable to affect significantly the fluid packets farther off the wall in the final approach to separation. In this particular case, the viscous action arrives even too late to have a substantial influence on the developing separation, as the separation center ($\xi_s \approx 1.55$, $\eta_s \approx 0.55$) is essentially unchanged. A similar explosion between $t = 3.35$ and $t = 3.38$ is found in Fig. 9 where the decelerated motion is triggered at $t_1 = 1.5$. Because of the advance in trigger time, we find a new separation center ($\xi_s \approx 1.30$, $\eta_s \approx 0.68$). Thus a different fluid packet is now responsible, through its deformation, for separation.

B. Simultaneous Translation and Pitching

In this study a pitching motion is added simultaneously to the original impulsively started translation. The purpose is to simulate the initial separation when the airfoil goes into dynamic stall by pitching. The cylinder is of course only a crude caricature of real airfoil, but if leading-edge separation is the culprit, as generally believed, our model should shed much light on the complex flow behavior leading to separation.

See again Fig. 2, where the cylinder motion is specified as a forward velocity U_A and a rotation of angular velocity Ω (positive counterclockwise) about the pivot point, which lies off center with an eccentricity e as defined in the sketch. If both U_A and Ω are constant after an impulsive start, the instantaneous tangential velocity $U(x,t)$ along the surface, as viewed from the body-fixed coordinates, is found to be, after setting the speed to equal U_0 (the standard value)

$$U = 2U_0 \sin(\Psi - \theta) + \Omega(1 + 2e \cos\Psi) \tag{15}$$

This then is the relative velocity needed to compute the boundary-layer flow in moving axes for the present problem. It may be converted to an effective pressure gradient to interpret the boundary layer as if in an inertial frame.

A technical problem of integrating the unsteady boundary-layer equations arises in algorithms that make use of the velocity profile at the stagnation point to construct the flow by marching downstream. In general, the stagnation point is nonstationary, and ad hoc treatments may be necessary; see, e.g., Cebeci and Carr[18] and Geissler.[19] We choose to eliminate the dependence on the stagnation point, which is a priori unknown in the general case. This is achieved by formulating strictly an initial-value problem for the entire boundary layer over the circular cylinder, with periodical boundary conditions in the circumferential direction. The computation domain for the whole circular cylinder has the range $0 \le \Psi \le 2\pi$, rather than just the upper half of it ($0 \le \Psi \le \pi$) as was considered in the preceding section. The procedure has been successfully tested in the standard impulsively started cylinder problem for which the stagnation points are fixed. Symmetry of the flow was not assumed but well captured by the new program.

The results for two values of Ω, −0.1 and −0.5, and three values of eccentricity e, 0.0, −0.4, and −0.8, are summarized

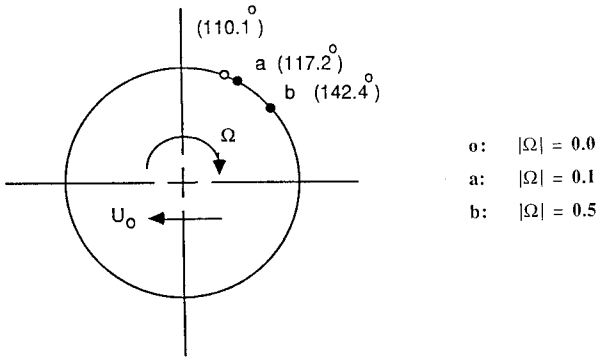

Fig. 10 Streamwise position of the separation point as viewed from the reference frame fixed to the translational motion of the cylinder.

in Table 2. If the standard case of $\Omega = 0$, first obtained by van Dommelen and Shen,[10,11] is used as the reference, the limited data now cover a matrix of $\Omega = 0$, -0.1, -0.5 and $e = 0$, -0.4, -0.8. They at least provide a glimpse of the effects of constant Ω with different pivot locations and of constant pivot location e but at different rotational speeds. For each combination of Ω and e, we have calculated (with a mesh of $65 \times 65 \times 0.025$) the separation center (ξ_s,η_s), the separation time t_s, the separation location x_s along the surface, as well as the instantaneous local speed u_s of the separation point. Calculations were terminated at the first appearance of separation, which could occur at either the upper or the lower surface. Note that the streamwise locations are measured from the fixed leading edge, point A at $t = 0$ (see Fig. 2).

The case of $e = 0$ and Ω fixed is of course the transient problem of the rotating cylinder in forward motion, impulsively started from rest. Note that in usual treatments, the parameter of rotational motion is specified through the sur-

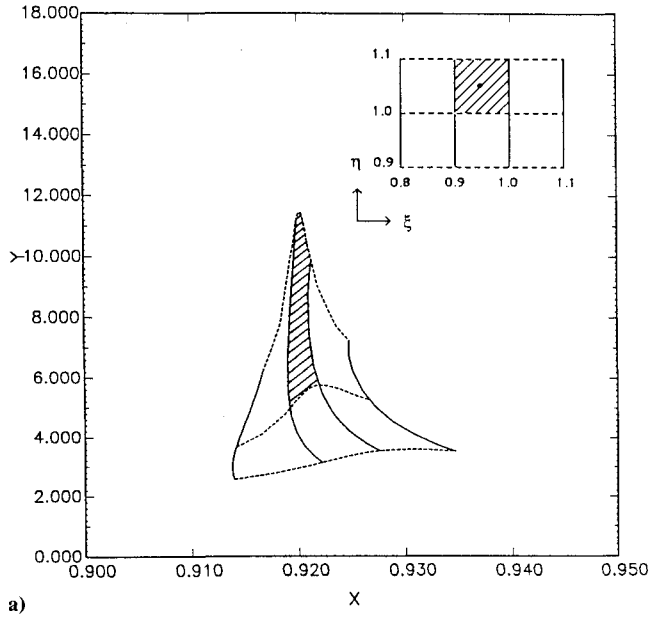

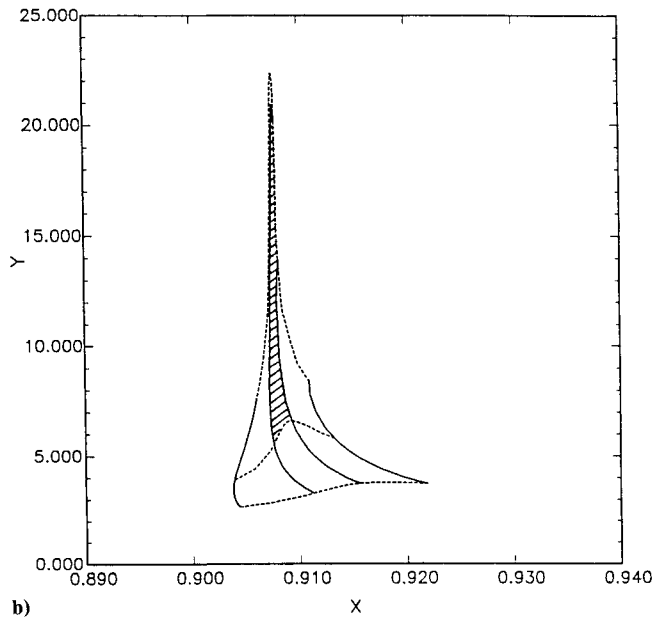

Fig. 11 Deformation of fluid packet close to separation; $\Omega = -0.5$, $e = 0.0$: a) $t = 3.15$; b) $t = 3.17$.

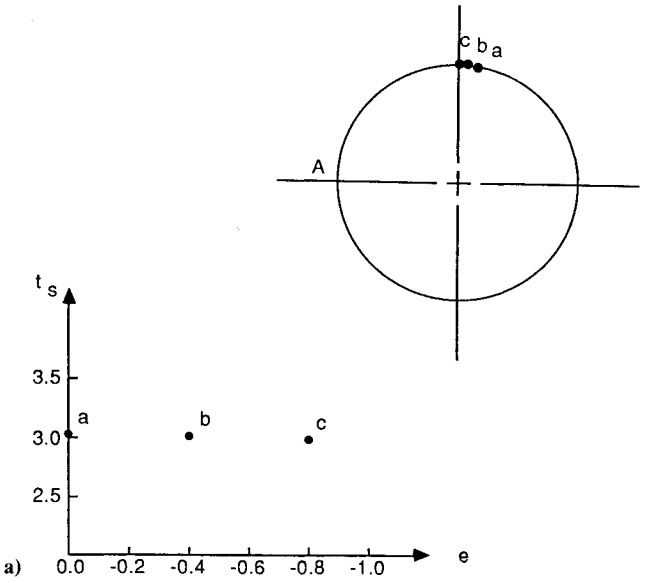

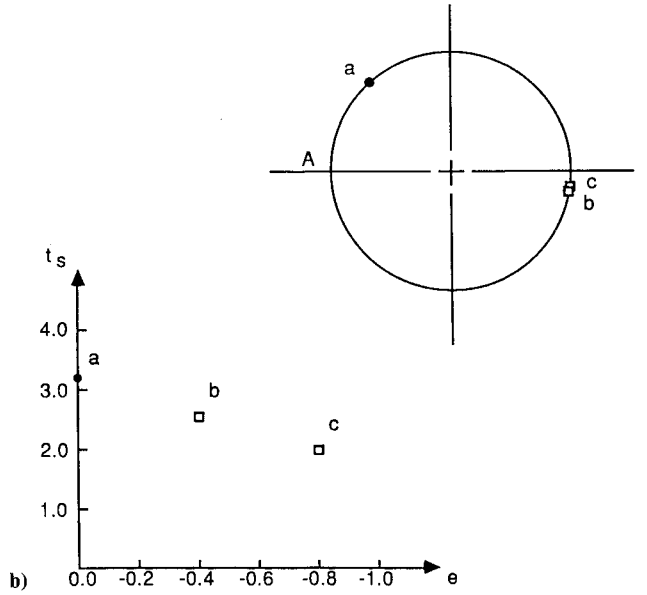

Fig. 12 Effects of changing the pivot location on the separation time and the streamwise position of the separation point as viewed from the reference frame fixed to the cylinder: a) $\Omega = -0.1$; b) $\Omega = -0.5$.

face velocity—as a moving wall. We remind readers also that our results contain the angular displacement of the body-fixed leading edge A. The predicted effects of rotational speed on the location of initial appearance of separation are then shown in Fig. 10. Indeed, the separation point does shift in the direction of the moving wall, and more so at larger wall velocity, very much like in the steady case. However, the correspondence may be fortuitous. Furthermore, after t_s, position of the separation point continues to move before eventually reaching the steady-state location. The boundary-layer equations, obviously, cannot be relied on beyond the onset of separation. Since our solution describes the evolution of the boundary layer over the entire circular cylinder, no attempt was made to calculate the separation on the lower surface over which the boundary layer remained attached until $t = t_s$. The behavior of fluid packets near separation is presented in Fig. 11. A similar explosive structure as previously found in linear acceleration cases is once more exhibited.

The position of the separation point under various pivot locations, as measured from the body-fixed leading edge A, is graphically presented in Fig. 12. The result shows a weak dependence of the separation location on the pivot location when the rotation is small ($\Omega = -0.1$). As for the time of separation, at the smaller rate of pitch up ($\Omega = -0.1$), separation appears first on the upper surface at approximately $t_s = 3$ for all the pivot locations—perhaps because of the rather small angular displacement (17 deg) during this interval. Consistent with this interpretation is also the fact that the fluid packet causing separation is nearly the same for the two pivot locations ($\xi_s = 1.31$, $\eta_s = 0.59$ for $e = -0.4$ and $\xi_s = 1.25$ and $\eta_s = 0.59$ for $e = -0.8$). A different picture emerges for the larger pitch rate. Separation now first appears on the lower surface for both $e = -0.4$ and $e = -0.8$, and the separation time is found to be advanced as the pivot location shifts toward the leading edge. However, the fluid packet causing separation is again only slightly influenced by the pivot location.

IV. Conclusions

The recent interest in rapidly maneuvering aircraft brings into sharp focus the long neglected topic of fluid mechanics as observed in a noninertial frame, in particular the body-fixed coordinates commonly used in rigid dynamics. As separated flows clearly rank among the main issues in application, we need to deal squarely with the Naiver-Stokes equations, now amended with several body-force terms. The latter can appear in various combinations to produce a multitude of heretofore unfamiliar, hence confusing, flow behaviors. In the boundary-layer approximation, the three-dimensional problem in body-fixed coordinates is found to obey essentially the same equations as the usual case in an inertial frame, provided the pressure gradient is explicitly expressed in terms of the freestream velocity distribution. The only additional feature due to the body motion is the Coriolis effect, proportional to the component, normal to the local body surface, of the angular velocity of body motion. We anticipate, therefore, novel features to reveal themselves in future research on separated flows on such objects as helicopter blades, propellers, cascades, and rapidly turning aircraft.

For two-dimensional bodies in plane motion, the Coriolis term does not appear, and the boundary-layer problem is no different from the usual case. The earlier Lagrangian program for a circular cylinder impulsively started into constant-speed forward motion due to van Dommelen[11] is basically applicable. It has been adapted to calculate the boundary layer over the entire body surface with unknown moving stagnation points. The boundary-layer calculation pinpoints the time and locality of the first appearance of separation. Effects of acceleration and deceleration of the forward motion and those from simultaneous pitching about an off-center pivot, have been determined for a range of the relevant parameters. The results do show some systematic trends but defy simplistic generalization. Some may even be puzzling to those with vast experience of specific quasi-stationary behaviors involving well-developed separation. Our results deal with the first appearance of separation; they must not be so interpreted. There should be no controversy that concepts based on the effective pressure gradient and wall shear distribution, at any given instant, are insufficient to provide generally valid correlations with unsteady separation. A challenge to all is how to characterize the time history properly and effectively for applications to rapidly changing body motions.

In the Lagrangian viewpoint, the boundary-layer singularity physically depicts the creation of a virtual barrier by a certain fluid *packet*, which gets to be squeezed into a slice of zero thickness in the streamwise direction. The progress toward separation is therefore tied in with the developing deformation of the fluid packet along its trajectory. (The instantaneous streamline pattern provides, for this purpose, at best only partial information.) It seems possible to alter the courses of potentially separation-prone fluid packets through body motion or active control devices. But a certain response time is necessary. Furthermore, when the body changes its motion or the control device is activated, the inviscid pressure disturbances are immediately felt by the fluid packet; while the viscous effects from the tangent stresses at the body surface must be subject to more time lag. A better understanding of the underlying mechanism should be helpful in attempts to promote or delay separation on maneuvering bodies.

Acknowledgments

This work was partially supported by Air Force Office of Scientific Research Contract AFOSR-86-0328. The numerical calculation was performed by using the Cornell National Supercomputer Facility, a resource of the Center for Theory and Simulation in Science and Engineering, which receives major funding from the National Science Foundation and IBM Corporation, with additional support from New York State and members of the Corporate Research Institute.

References

[1]Ericsson, L. E., "A Critical Look at Dynamic Simulation of Viscous Flow," *Unsteady Aerodynamics—Fundamentals and Application to Aircraft Dynamics*, AGARD CP No. 386, Nov. 1985.

[2]Ericsson, L. E., "Dynamic Omnipresence of Moving Wall Effects, a Selected Review," AIAA Paper 87-0241, June 1987.

[3]Sears, W. R., and Telionis, D. P., "Boundary Layer Separation in Unsteady Flow," *SIAM Journal of Applied Mathematics*, Vol. 28, No. 1, 1975, pp. 215–235.

[4]Telionis, D. P., "Boundary Layer Separation," Ph.D. Thesis, Cornell Univ., Ithaca, NY, 1970.

[5]Ericsson, L. E., and Reding, J. P., "Fluid Mechanics of Dynamic Stall. Pt. I: Unsteady Flow Concepts," *Journal of Fluids and Structures*, Vol. 2, Jan. 1988, pp. 1–33.

[6]Ericsson, L. E., "Moving Wall Effects in Unsteady Flow," *Journal of Aircraft*, Vol. 25, No. 11, 1988, pp. 977–990.

[7]Jumper, E. J., "Mass Ingestion: Perturbation Method Useful in Analyzing Some Boundary-Layer Problems," American Society of Mechanical Engineers, Paper 86-WA/FE-10, Dec. 1986.

[8]Jumper, E. J., Hitchcock, J. E., Lawrence, T. S., and Docker, R. G., "Investigating Dynamic Stall Using a Modified Momentum Integral Method," AIAA Paper 87-0431, June 1987.

[9]Shen, S. F., "Considerations for Analyzing Separated Flows over Arbitrarily Maneuvering Bodies," Air Force Office of Scientific Research Workshop on Unsteady Separated Flows, Colorado Springs, CO, July 1987.

[10]van Dommelen, L. L., and Shen, S. F., "The Spontaneous Generation of the Singularity in a Separating Boundary Layer," *Journal of Computational Physics*, Vol. 38, No. 2, 1980, pp. 125–140.

[11]van Dommelen, L. L., "Unsteady Boundary Layer Separation," Ph.D. Thesis, Cornell Univ., Ithaca, NY, 1981.

[12]Shen, S. F., "Some Considerations on Laminar Stability of Time-Dependent Basic Flows," *Journal of the Aeronautical Sciences*, Vol. 28, No. 5, 1961, pp. 397–405.

[13]Fales, E. N., "A New Laboratory Technique for Investigation of

the Origin of Fluid Turbulence," *Journal of the Franklin Institute*, Vol. 259, No. 6, 1955, pp. 491–515.

[14]Fogarty, L. E., "The Laminar Boundary Layer over a Rotating Blade," *Journal of the Aeronautical Sciences*, Vol. 18, No. 4, 1951, pp. 247–252.

[15]Tan, H. S., "On Laminar Boundary Layer over a Rotating Blade," *Journal of the Aeronautical Sciences*, Vol. 20, No. 11, 1953, pp. 780–781.

[16]Matsushita, M., Murata, S., and Akamatsu, T., "Studies on Boundary-Layer Separation in Unsteady Flow Using an Integral Method," *Journal of Fluid Mechanics*, Vol. 149, Dec. 1984, pp. 477–501.

[17]Shen, S. F., "Unsteady Separation According to the Boundary Layer Approximation," *Advanced Applied Mechanics*, Vol. 18, 1978, pp. 177–219.

[18]Cebeci, T., and Carr, L. W., "Calculation of Boundary Layers near the Stagnation Point on an Oscillating Airfoil," NASA TM 84305, May 1983.

[19]Geissler, W., "Unsteady Boundary-Layer Separation on Airfoils Performing Large-Amplitude Oscillations-Dynamic Stall," *Unsteady Aerodynamics—Fundamentals and Application to Aircraft Dynamics*, AGARD CP No. 386, Nov. 1985.